Monthly Notices
of the
ROYAL ASTRONOMICAL SOCIETY

MNRAS **433,** 928–934 (2013)
Advance Access publication 2013 June 14

doi:10.1093/mnras/stt765

Dynamical analysis of the Gliese-876 Laplace resonance

J. G. Martí,[1]⋆ C. A. Giuppone[1,2] and C. Beaugé[1]

[1]*Universidad Nacional de Córdoba, Observatorio Astronómico, IATE, Laprida 854, X5000BGR Córdoba, Argentina*
[2]*Departamento de Física, I3N, Universidade de Aveiro, Campus de Santiago, P-3810-193 Aveiro, Portugal*

Accepted 2013 May 1. Received 2013 April 30; in original form 2013 April 19

ABSTRACT

The number of multiple-planet systems known to be involved in mean motion conmensurabilities has increased significantly since the *Kepler* mission. Although most correspond to two-planet resonances, multiple resonances have also been found. The Laplace resonance is a particular case of a three-body resonance in which the period ratio between consecutive pairs is $n_1/n_2 \sim n_2/n_3 \sim 2/1$. It is not clear how this triple resonance acts to stabilize (or not) the system.

The most reliable extrasolar system located in a Laplace resonance is GJ 876, because it has two independent confirmations. However, best-fit parameters were obtained without previous knowledge of resonance structure, and not all possible stable solutions for the system have been explored.

In the present work we explore the various configurations allowed by the Laplace resonance in the GJ 876 system by varying the planetary parameters of the third outer planet. We find that in this case the Laplace resonance is a stabilization mechanism in itself, defined by a tiny island of regular motion surrounded by (unstable) highly chaotic orbits. Low-eccentricity orbits and mutual inclinations from -20° to 20° are compatible with observations. A definite range of mass ratio must be assumed to maintain orbital stability. Finally, we provide constraints on the argument of pericentres and mean anomalies to ensure stability for this kind of system.

Key words: techniques: radial velocities – celestial mechanics – planets and satellites: formation.

1 INTRODUCTION

A three-body resonance occurs in a planetary configuration in which the period ratios between consecutive pairs of planets satisfy $n_1/n_2 \sim p/q$ and $n_2/n_3 \sim r/s$, with $p, q, r, s \in Z$. Because of the success of the *Kepler* mission in detecting exosystems (candidates) trapped in three-body resonances and because this type of multiresonant configuration provides a possible origin for the giant planets of our own Solar system (Morbidelli et al. 2007), three-body resonances are currently of special interest in the scientific community.

Among the systems with three-planet resonances, Lissauer et al. (2011) found a number of *Kepler* candidates in multiresonant configurations (e.g. KOI-152, KOI-730 and KOI-500). KOI-152 is a system of three hot super-Earth candidates that are in (or near) a 4:2:1 mean motion resonance (MMR) (Wang, Ji & Zhou 2012), having transit time variation (TTV) signals that correspond to gravitational interactions between them. The four candidates in the KOI-730 system satisfy the mean motion ratio 8:6:4:3. This resonant chain is a potential missing link that explains how planets that are subject to migration in a gas or planetesimal disc can avoid close encounters with each other, being brought to a very closely packed, but stable, configuration (Lissauer et al. 2011). KOI-500 is a (near-)resonant five-candidate system with combinations of mean motions given by $2n_2 - 5n_3 + 3n_4 \sim 1.6 \times 10^{-5}$ and $2n_3 - 6n_4 + 4n_5 \sim 1.3 \times 10^{-5}$, perhaps suggesting a strong interaction owing to hidden companions in MMR (Lissauer et al. 2011). On the other hand, numerical studies using Saturn, Uranus and Neptune masses from Morbidelli et al. (2007) showed that it is possible to obtain configurations for which the period ratios between consecutive pairs, namely 2:3 and 4:5 (or 3:4), are stable for 400 Gyr.

The case for which the period ratio between consecutive pairs is $n_1/n_2 \sim n_2/n_3 \sim 2/1$ is a particular type of three-body resonance termed the *Laplace resonance*. This configuration is rare in our own Solar system, and the Galilean satellites Io, Europa and Ganymede constitute the only known example of such a configuration (Ferraz-Mello 1979). Among the vast variety of extrasolar planets, only GJ 876 has been confirmed to be in a Laplace resonance.

Unconfirmed candidates of Laplace resonance detected with radial velocity can be found in HD 40307 and 82943. The system HD 40307 has been proposed to be locked in 4:2:1 MMR and has been studied by Papaloizou & Terquem (2010). HD 82943 has been

⋆E-mail: javi@oac.uncor.edu

studied by Beaugé et al. (2008). The mass ratio between the inner pair is $m_2/m_1 \sim 1$, and that between the outer pair is $m_3/m_2 \sim 0.2$. The results were found using a Stokes-like drag force with fixed values for the e-folding times for the semimajor axes and eccentricities. The authors tested a wide variety of masses for the third body, and the planets always evolved towards a double MMR, in which $n_1/n_2 \sim 2/1$ and the ratio n_2/n_3 corresponded to a ratio of integers. In the vast majority of simulations, the outer pair of planets was also trapped in a 2/1 MMR (i.e. $n_2/n_3 \sim 2/1$). A dynamical analysis of the results revealed that there is an asymmetric libration of resonant angles. Finally, an observation that could be useful in this analysis is that the phase space associated with the Laplace resonance is complex, and appears to be populated with a number of small islands of stable motion surrounded by large chaotic regions of instability (see fig. 9 bottom in Beaugé et al. 2008).

The goal of the present work is to develop a dynamical analysis of the Laplace resonance using as the primary target GJ 876. This system has been discussed in several works, giving us the posibility to compare our results with previous ones. In a parallel way, we extend our understanding of the dynamical complexities of the Laplace resonance.

2 GJ 876

The GJ 876 system contains four confirmed planets, and, as an exoplanetary system, is unique. GJ 876 was the first system detected to be locked into a MMR. The planets GJ 876 b and c have a mass ratio $m_c/m_b \sim 3$ and orbital periods of 61.11 and 30.08 d, respectively (Rivera et al. 2010), and their strong interaction is evident in the radial velocity because of their small semimajor axis (<0.2 au) and low-mass primary star ($M_* = 0.32 M_\odot$ for Rivera et al. 2010 and $M_* = 0.334\ M_\odot$ for Baluev 2011). An extensive bibliography on this system brought major contributions to the development of models and methods, including: detection using mutual interaction (Rivera & Lissauer 2000; Laughlin & Chambers 2001), planetary migration and resonance capture (Kley et al. 2005), and periodic motion in planetary resonances for massive planets (Hadjidemetriou 2002; Beaugé & Michtchenko 2003).

From the very beginning, the possibility of this system hosting additional planetary bodies has been the subject of intense studies, and the last and outermost planet (GJ 876 e) was confirmed by two independent works (Rivera et al. 2010; Baluev 2011) to be in a three-body resonant configuration (e.g. Laplace resonance) with planets GJ 876 c and b. A detailed stability analysis for the system containing an additional planet with a period of 15 d showed that this configuration was discarded (Correia et al. 2010; Gerlach & Haghighipour 2012).

2.1 Resonant variables

Consider a system with three planets in the Laplace configuration. Then, the resonant variables involved in this problem are the resonant angles of the two two-body resonances taken separately:

$$\theta_1 = \lambda_1 - 2\lambda_2 + \varpi_1,$$

$$\theta_2 = \lambda_1 - 2\lambda_2 + \varpi_2,$$

$$\theta_3 = \lambda_2 - 2\lambda_3 + \varpi_2,$$

$$\theta_4 = \lambda_2 - 2\lambda_3 + \varpi_3, \qquad (1)$$

where λ is the mean longitude and ϖ is the argument of the pericentre. We reserve the subscripts 1 to 3 for orbital elements and masses from the innermost to the outermost planet involved in the Laplace resonance.

We can also define the Laplace variable (or θ_5), which can be written as a combination of two of the resonant angles:

$$\theta_5 = \theta_2 - \theta_3 = \lambda_1 - 3\lambda_2 + 2\lambda_3. \qquad (2)$$

The secular variables are:

$$\Delta\varpi_{21} = \varpi_2 - \varpi_1 = \theta_2 - \theta_1,$$

$$\Delta\varpi_{32} = \varpi_3 - \varpi_2 = \theta_4 - \theta_3. \qquad (3)$$

The libration/circulation regime and libration amplitudes of these angles provide much information about the resonant dynamics. It is clear from equation (2) that a simultaneous libration of the angles θ_2 and θ_3 means that the Laplace angle is also librating.

Simplified dynamical models for this type of resonant configuration can be found in Lithwick & Wu (2012) and Batygin & Morbidelli (2013). These models were obtained as a way of introducing dissipative effects in the evolution of resonant configurations, and are too simplified for a general dynamical analysis of three-body resonances. However, numerical simulations of capture into the Laplace resonance owing to gas-driven migration were performed in Libert & Tsiganis (2011), for various mass ratios and drag parameters. The results show that if one of the inner planets has its eccentricity pumped to a value higher than 0.3, then the mutual inclination can be excited up to 30°.

We use here the best-fit model for GJ 876 as a first step in trying to understand this Laplace resonance configuration.

2.2 Dynamics for best fits

Table 1 gives the best-fit planetary masses and orbital parameters from Rivera et al. (2010) and Baluev (2011) (RI10 and BA11 respectively hereafter). The inner pair has an inner planet significantly less massive than the outer (e.g. GJ 876 $m_b/m_c \sim 3$); while for the outer pair, the mass ratio is $m_e/m_b \sim 0.02$. We integrated the initial conditions from Table 1 and obtained qualitatively the same results as RI10 and BA11.

The libration centres (around zero) and amplitudes are similar for the angles θ_1, θ_2 and θ_3, while the last of the resonant angles θ_4 is librating around 180° with the same amplitude for both published solutions. This last result differs slightly from results given in RI10, who claim that θ_4 is circulating. Some values for $\theta_4 \sim 0°$ due to the small eccentricity of the planet, thus apparently giving circulation instead of libration around $\theta_4 = 180°$.

The initial conditions from RI10 are plotted in $(e_j \sin\theta_i, e_j \cos\theta_i)$ space in Fig. 1. Colour codes are used for different total integration times: 10^2 yr (light green), 10^3 yr (dark green), 10^4 yr (light blue), and 10^5 yr (dark blue). The blue dots cannot be seen because no change in the libration region is evident after the first 10^3 yr. We checked that the secular angles $\Delta\omega_{32}$ and $\Delta\omega_{31}$ librate around 180°, while $\Delta\omega_{21}$ librates with a very low amplitude around zero (the same behaviour as found by RI10 and BA11).

The Laplace angle θ_5 librates around zero with an amplitude ~40° (i.e. $\theta_5 = 0 \pm 40°$) for at least 3×10^6 yr in both published fits. This amplitude is also consistent with the value given in RI10. The non-regular libration of the Laplace angle is evident in the first 100 yr of integrations.

We integrated the two solutions listed in Table 1, including calculations of various chaoticity indicators, which identified this systems as irregular. This chaotic nature of the systems is discussed later and analysed in more detail in Sections 2.3 and 3. Although

Table 1. Four-planet coplanar fits for GJ 876 with $i = 56.^{\circ}1$ for Baluev (2011) and with $i = 59.^{\circ}0$ for Rivera et al. (2010). The masses listed in the table are corrected by the corresponding value of the inclination for each fit. The coordinates are given in the Jacobi reference frame. In his work, Baluev gives the angle $\psi = M + \omega$, so the calculated value of M is also given here (in the same way as Baluev 2011).

	Best fit for Baluev (2011)				Best fit for Rivera et al. (2010)			
Parameter	Planet d	Planet c	Planet b	Planet e	Planet d	Planet c	Planet b	Planet e
P (days)	1.937886	30.1829	60.9904	124.51	1.937780	30.0881	61.1166	124.26
m ($M_{\rm Jup}$)	0.0218	0.747	2.337	0.0482	0.0214	0.7142	2.2756	0.0459
a (au)	0.02110625	0.131727	0.211018	0.33961	0.02080665	0.129590	0.208317	0.3343
e	0.178	0.2498	0.0328	0.008	0.207	0.25591	0.0324	0.055
ω ($^{\circ}$)	224.0	252.08	248.7	181.0	234.0	48.76	50.3	239.0
ψ ($^{\circ}$)	357.6	71.09	341.13	299.3	229.0	343.35	16.0	234.0
M ($^{\circ}$)	133.6	179.01	92.43	118.3	355.0	294.59	325.7	335.0

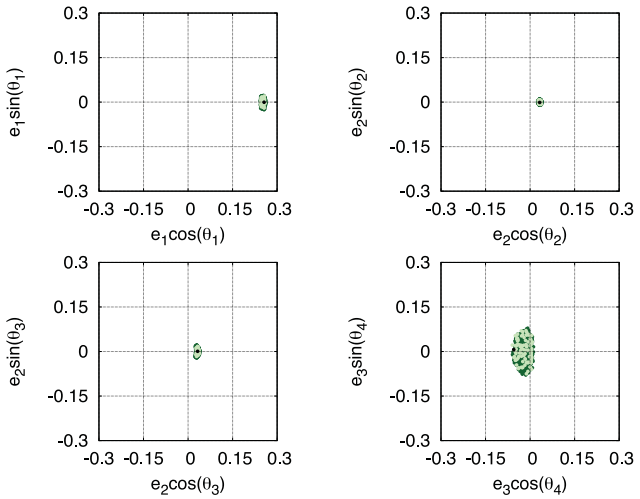

Figure 1. Time evolution of the resonant angles θ_i, $i = 1, 2, 3, 4$, for our integration, with initial conditions taken from Rivera's fit.

chaotic, both systems are long-term stable, and it is worthwhile to analyse them in a thorough way.

Rivera and Baluev showed that their solutions are stable for at least 10^6 yr. These long-term integrations contain thousands of secular periods of the system, corresponding to roughly 10^8 to 10^9 yr when rescaled to the subsystem of the giant planets in our Solar system. Baluev's long-term integrations were performed with initial conditions slightly different from those listed in Table 1. The parameters were determined with the fitting model that accounts for the white and red noise and fixing the eccentricity of the outermost planet at $e_{\rm e} = 0$. In addition, long-term integrations were performed with only three planets, not taking into account the innermost planet.

2.3 Dynamics around best fits

Throughout the numerical integrations we choose the mass of the central star according to each fit; in the case of RI10 $M_* = 0.32\,{\rm M}_\odot$, while in BA11 $M_* = 0.334\,{\rm M}_\odot$. The integrations are for coplanar systems; however, we checked some runs with nearly coplanar systems and the general results were almost unaltered.

As mentioned in the previous section, the best fits resulted in chaotic but long-term stable systems. This led us to question the behaviour of the system surrounding the best fits. The dynamics of the Laplace resonance present in GJ 876 is studied in this work through several stability maps carried out with a Burlisch–Stoer-based N-body code (precision better than 10^{-12}) using Jacobi osculating variables as initial conditions.

The numerical integrator calculates the MEGNO (mean exponential growth of nearby orbits) value for each initial condition. For a detailed explanation of MEGNO ($\langle Y \rangle$) see Cincotta & Simó (2000), Cincotta, Giordano & Simó (2003) and Maffione et al. (2011). This indicator has the useful feature that it identifies chaotic orbits in less CPU time than other indicators (e.g. the Lyapunov characteristic exponent); however, it cannot give a precise representation of the structure of a resonance, as it only differentiates regular ($\langle Y \rangle \sim 2$) from chaotic ($\langle Y \rangle \gg 2$) orbits.

For each initial condition we also calculated the maximum amplitude of variation of eccentricity attained during the integration (Δe_i for each planet). Owing to the conservation of angular momentum, the lower-mass planet exhibits higher variation ($\Delta e_3 > \Delta e_2, \Delta e_1$). This indicator discriminates different kinds of dynamics of the system. The most drastic change in the eccentricity of a planet is when the body is located near the separatrix of a resonance, although the amplitude of variation has an upper bound. Thus Δe_3 can be used to define precise limits to resonance widths and extensions, without expensive additional numerical calculations.

We used these two indicators because they are complementary and provide different kinds of information.

2.4 Chaoticity maps

We derived a series of maps around Rivera's solution from Table 1 to find information regarding the observed stability/chaos in the GJ 876 system. We first integrated a grid of initial conditions for the outermost planet in the (a_3, e_3) plane, taking its mass equal to $14.6 M_\oplus$. Fig. 2 shows the results in the region $a \in (0.03, 4.86)$ and $e \in (0.0, 0.4)$. The colours show the (a)MEGNO and (b)Δe_3 values of each initial condition integrated for 5×10^4 yr. We identify the locations of planets 1 and 2 with white circles and the nominal location of planet 3 with a black circle. Red colour codes are reserved for orbits that disrupt within the total integration time.

Probably the first insight into the stability of the system can be obtained by testing whether the system is stable according to the stability criteria developed by Marchal & Saari (1975). This criterion uses the energy and angular momentum of a three-body system to estimate the Hill-stability limit. The problem of trying to fit this limit to our system is that we have essentially a four-body system. It is also a criterion developed considering the secular evolution of the system, which is not the case for a system trapped in MMRs. With these reservations in mind, we have plotted the

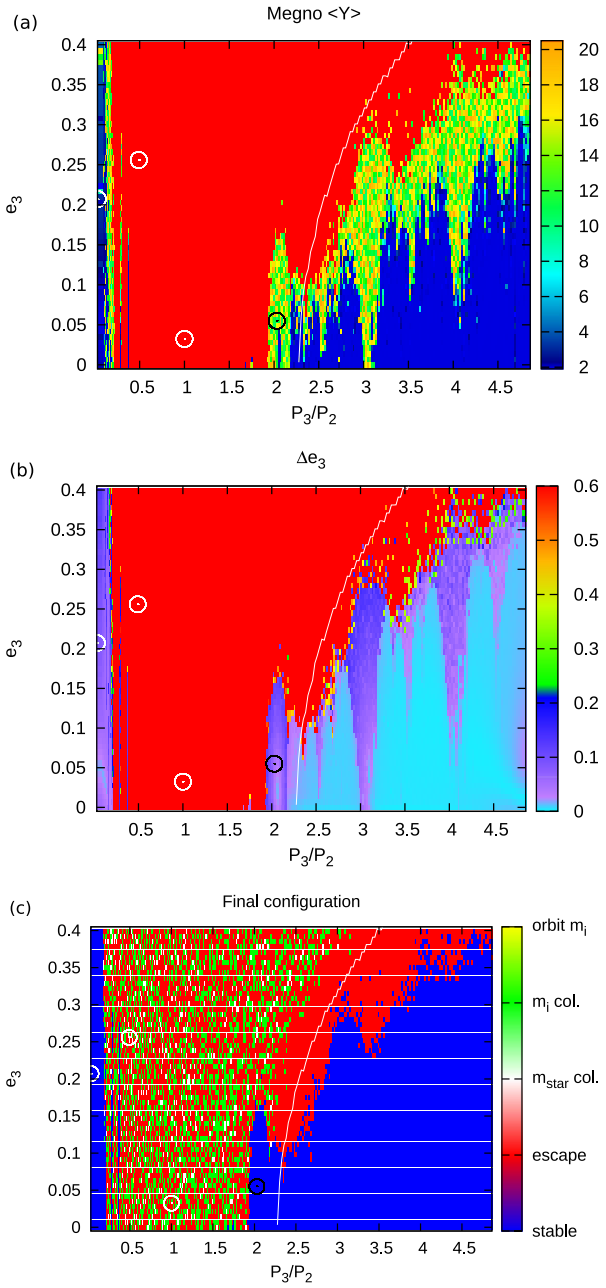

Figure 2. Stability maps for an exterior planet in Laplace resonance. (a) MEGNO chaos indicator; (b) Δe_3; (c) test-planet end-states: stable, escape from system ($a_3 > 5$ au), collision with central star M_* ($a_3 < 0.05$ au), collision with another companion (when the distance with any other planet is lower than the sum of their mutual radii), and capture orbit around m_i. The white line was calculated using Gladman (1993). White circles are the locations in the plane for planets 1 and 2. The phase space of the system is explored by varying the semimajor axis a and eccentricity e of the outer planet, marked as a black circle.

analytical stability limit as a white curve. The agreement with the *N*-body simulations is not clear.

Although these maps were derived using Rivera's best fit, similar maps were also derived using Baluev's best fit. The results are almost independent of the fit used for the GJ 876 system, probably evidencing the robustness of this approach.

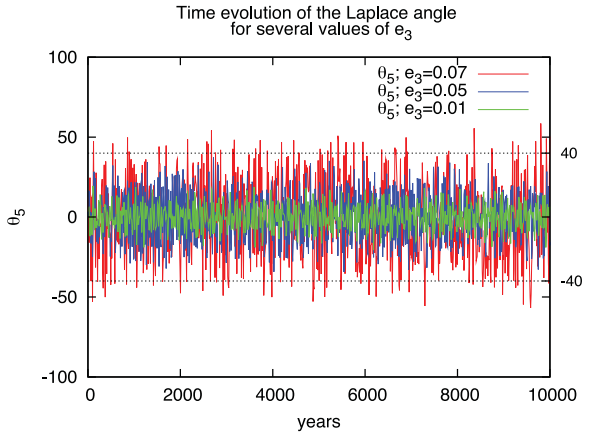

Figure 3. Evolution of the Laplace angle for various values of the initial eccentricity of the exterior planet. It seems that $e_3 \sim 0.015$ gives the minimum amplitude for the oscillation.

The MEGNO colour-code identifies the location of Rivera's best fit inside a chaotic island (Fig. 2a). Not surprisingly, because the best-fit configuration has a chaotic value of MEGNO, this island appears to be surrounded by highly unstable regions. The x-axis was rescaled in order to show the period ratio P_3/P_2, and enable easy identification of the vertical spikes at the true locations of several MMRs; namely from left to right 2:1, 5:2, 3:1, 7:2, 4:1 and 9:2. MEGNO identifies all the resonances as chaotic. When we plot the same grid using a colour-code for the variation of eccentricity (Fig. 2b) the MMR structure can be seen more clearly. Outside the MMRs, the eccentricity variation of the exterior planet remains almost unaltered ($\Delta e_3 \sim 0$), while inside the MMRs, variations of the order of $\Delta e_3 \lesssim 0.2$ are observed. When two isolated resonances overlap each other the system becomes unstable, explaining the origin of the red region below the Marchal & Saari (1975) limit. Fig. 2(c) shows the test planet final states (stable, escape, collision or capture). All the unstable conditions in red located to the right of the white line calculated with the criteria of Marchal & Saari (1975) correspond to orbits that escape from the system, and are thus Hill-stable configurations. Initial conditions to the left of this line can have several final states; however, capture around the other planets seems to be improbable, possibly owing to the strong interactions between the inner pair of planets involved in the Laplace resonance.

In Fig. 2(a) we can see a strip located at almost the nominal semi-major axis but for eccentricity around $e_3 \sim 0.03$ where MEGNO values are equal to 2 (regular orbits) and $\Delta e_3 \sim 0$. Thus we identify this strip as the probable centre of the resonance for this system. We integrated several conditions in this strip to show how the amplitude of the Laplace angle varies. Fig. 3 shows the variation of θ_5 with time for three of these runs. It clearly shows the tendency of the Laplace angle libration amplitude to go to zero for values around $e_3 = 0.015$.

As stated above, although the best fits of Table 1 are catalogued as chaotic, this first sight of the phase space surrounding the initial condition for the best fit can provide some clues on the long-term stability of the Laplace resonance of GJ 876. In fact, the location of the outermost planet best fit relative to this regularity strip at the 2:1 MMR with planet 2 is probably causing the system to be long-term stable, despite its chaotic nature.

Three-body resonances are much more complex than their two-body counterparts. There are more free parameters to sample in the

maps. Thus, we proceeded to analyse other planes to gain further insight.

Because the pair eccentricity and argument of perihelion (e_3, ω_3) are strongly correlated and not very well constrained from radial velocity determinations (see e.g. Giuppone et al. 2009), it is expected that the GJ 876 system will have a lack of precision in those two parameters. Thus we performed a search within the plane (e_3, θ_4) to see if we could find a regular solution throughout the resonant angle $\theta_4 = \theta_4(\omega_3)$.

We derived (e_3, θ_4) maps for Rivera's and Baluev's fits, and computed the values of $\langle Y \rangle$ and Δe_i, $i = 1, 2, 3$, as well as the disruption times of the original system. The stable island where the best fit from Table 1 is located is surrounded by a highly unstable region (not surviving after $\sim 10^3$ yr of integration) in red.

The results are shown in Fig. 4, where the value of Δe_3 is shown in colours (the MEGNO values for this map show that the region sampled does not exhibit regular dynamics). Despite this, we can see in Fig. 4 that the Δe_3 is a much better indicator of the dynamics of the system than other indicators. A structure of the space can clearly be distinguished, wherein, judging by the values for the total disruption times, the dynamics is stable for at least 10^5 yr. This island is present in both plots, top and bottom, and seems to differ in its orientation. Depending on the best fit, the orientation of the stable island seems to be (0°, 180°) for Rivera (Fig. 4a) or (90°, 270°) for Baluev (Fig. 4b). At the centre of this stable structure it can be seen that the orientation of the region with $\Delta e_3 \sim 0$ is similar to the outermost stable structure.

Finally, we must address the fact that the same results were obtained without considering the innermost planet (those with period $P \sim 1.93$ d), and thus there is no need to consider its presence as a chaoticity enhancer of the system. Owing to the similarity of results without planet d, we continued to work with only the three outermost planets of the GJ 876 system.

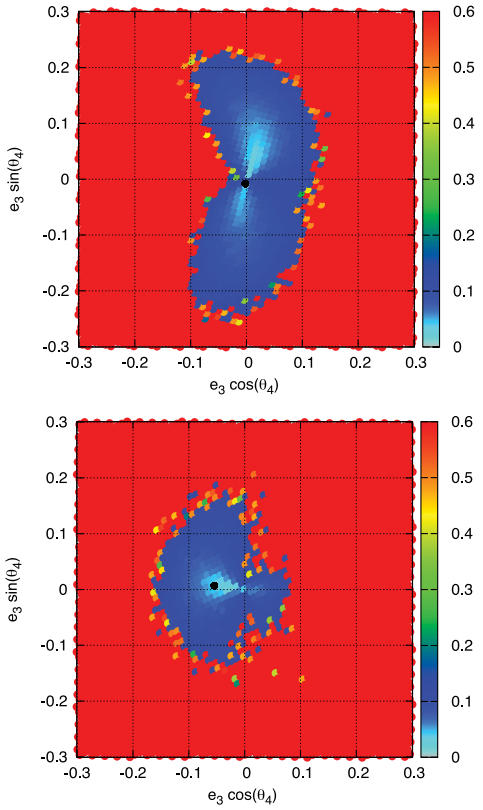

Figure 4. Δe_3 indicator for the exterior planet in the plane ($e_3 \cos\theta_4$, $e_3 \sin\theta_4$). (a) Baluev and (b) Rivera solutions for the GJ 876 system. The black dot represents the configuration from fits.

3 LIMITS TO THE STABILITY

In a more general view, we tested some stability (although not regularity) limits for a multiplanetary system locked in a Laplace resonance. We performed a series of runs on grids of initial conditions, varying the mass, inclination and eccentricity of the the outermost planet of the system GJ 876. We used the same chaoticity indicators as in the previous section. Although not significantly different, the grid evaluating the Δe_3 is the clearest because it shows very sharp limits for the long-term stability of the system.

First, we performed integrations of the GJ 876 configuration from Rivera's and Baluev's best fits, changing the mass of the exterior planet from 10^{-3} to $10 M_{\rm Jup}$ (i.e. corresponding to $m_3/m_2 \in (4 \times 10^{-4}$ to 4.2). Fig. 5(a) shows that there is a mass range in which we can have stable solutions trapped in a three-body Laplace configuration. There are no stable systems in a Laplace resonance with an infinitesimal outermost planet. As the mass of the exterior planet increases, the stronger interaction with the interior bodies causes the innermost planet eccentricity to vary up to 0.1. After $m_3/m_2 > 0.5$ (i.e. masses greater than 1.27 $M_{\rm Jup}$) the system no longer survives the 10^6 yr. We can see that the variation of the

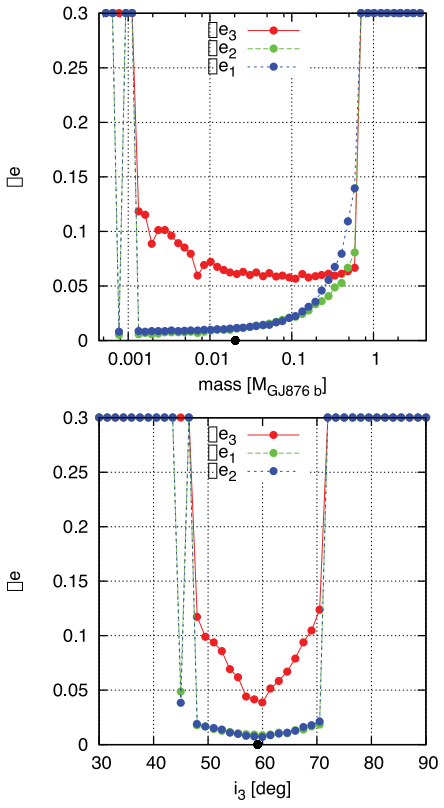

Figure 5. (a) Δe_i indicator for various masses of the exterior planet in units of the intermediate companion using Rivera's solution for the GJ 876 system. The black dot represents the configuration from fits. (b) Δe_i indicator for various inclinations of the exterior planet. Rivera's or Baluev's solution initial conditions give qualitatively the same results. The black dot represents 59°.

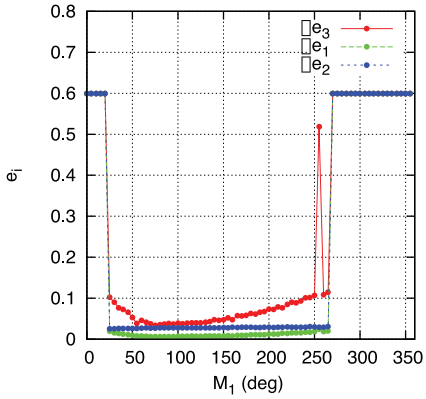

Figure 6. Δe_i indicator for various values of the mean anomaly of the exterior planet. These conditions were integrated for 1×10^6 yr, and it seems that the value of $M_1 = 60^\circ$ is the most regular condition.

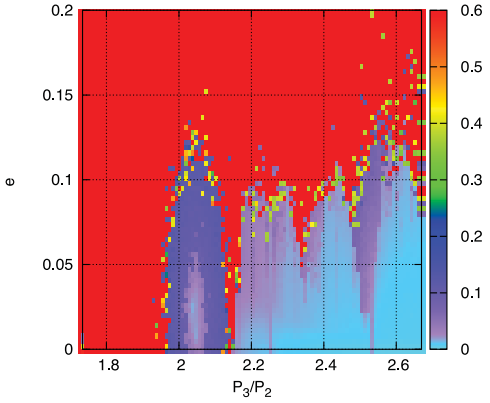

Figure 7. Representative plane showing the general dynamical properties of the Laplace resonance. The masses and eccentricities are taken from Table 1, and the angles are: $\theta_1 = \theta_2 = \theta_3 = \Delta\varpi_{31} = 0$, $M_3 = 60^\circ$ and $\Delta\varpi_{31} = 180^\circ$. All the conditions survived for more than 4×10^4 yr.

eccentricity of the exterior planet is compensated by the variation of the interior ones as its mass m_3 increases, and the perturbation increases.

Taking again the initial parameters from Table 1 we varied only the inclination of the exterior body, with the nodal longitude for all the planets set to 0°, and analysed the chaos/stability. Although chaotic, the system is stable for 10^6 yr for an inclination i_3 of the exterior planet from 46° to 72°, corresponding to mutual inclinations from −15° to 15°. Outside this range the system quickly collides (Fig. 5b). The minimum variation of eccentricity for the less massive planet is produced when the system is coplanar, and thus this is the most probable configuration. These results are also in agreement with Libert & Tsiganis (2011), who show that when eccentricities of the planets remain below ∼0.35, excitation of the inclinations does not occur.

To gain independence of initial values taken from Table 1, we found a representative plane in which all angles were set to 0° ($\theta_1 = \theta_2 = \theta_3 = \Delta\varpi_{31} = 0$) but $\Delta\varpi_{32} = 180^\circ$ (according to the results of long-term integrations). The only parameters with free values are the mean anomalies, which are related as $M_1 = 2M_2 = 4M_3$.

We integrated the systems using this representative plane, varying M_1 from 0° to 360° and using all other parameters as given in Table 1. Fig. 6 shows the variations of eccentricities Δe_i for the three planets depending on M_1, integrated for 10^6 yr. The other indicators showed the same behaviour. The aim of this M_1-grid was to identify the value of M_1 for which the system appears less chaotic in order to have a set of values for the angular parameters that are more suitable for analysing the stability maps of the system. All the systems are chaotic, but we identified very sharp limits to the long-term stability of the system: values of M_1 from 20° to 260° are long-term-stable for at least the total integration time-span. Because the system with $M_1 = 60^\circ$ exhibits the lower amplitude of variation of the eccentricity e_3, we accordingly chose the initial values of $M_2 = 120^\circ$ and $M_3 = 240^\circ$ and ran integrations in a (a_3, e_3) grid. We recall that unstable solutions for $M_1 \in [0^\circ, 20^\circ]$ as well as $M_1 \in [260^\circ, 360^\circ]$ are unstable in less than 10^5 yr.

Fig. 7 shows the final angle-independent representative plane for the Laplace resonance in the GJ 876 system. We can see the real extension of the Laplace resonance because we have become independent of the angles. An island of stability can be identified in the region where the MMR 2:1 is located, where the Laplace resonance is acting as a protection mechanism of the bodies. We also performed integrations of the individual 2:1 and 4:1 resonances with the two planets involved in each one. In the map of the 2:1 resonance the stability area shrinks much more than the area shown in Fig. 7. Thus the Laplace resonance can have important implications for the stability of extrasolar planetary systems, although this does not mean that every system trapped in a Laplace resonance will be stabilized by this mechanism.

4 CONCLUSIONS

Despite the arbitrary choice of the studied system (GJ 876), we introduced several constraints for a three-body system in a Laplace configuration. The analysis developed in this work could be easily expanded to any other system that seems to be near a three-body resonance.

We confirmed that published solutions of the system GJ 876 are located in a Laplace resonance, although their behaviour is chaotic (not due to the presence of the planet with period $P = 1.93$ d).

Not only is their Laplace angle librating with small amplitude, but the nominal locations of the systems from Table 1 are surrounded by stable although chaotic regions, as shown in Fig. 2. We also showed that the same systems when integrated in other planes (e.g. $\Delta\varpi = 180$) are stable. Regular solutions were found using Rivera's solution for e ranging from 0.01 to 0.05.

Through the exploration of the parameter space around best-fit solutions we found that other stable Laplace solutions exist, surrounded by unstable regions that are quickly evidenced in less than 1×10^3 yr. Furthermore, preferable orientations for the libration of Laplace angle were found (see Fig. 4).

We defined lower and upper mass limits for the outer planet ($0.02m_2 < m_3 < 0.5m_2$). We checked that these limits are independent of the mass ratio between the two inner planets. This independence suggests that similar stability limits can be found for other systems that are locked in this type of three-body configuration. Limits in the mass ratio could be very useful for future work on problems involving three-body resonances.

The mutual inclination for the exterior planet can be from −15° to −15°, with the coplanar orbits being more regular solutions.

The Laplace resonance is surrounded by chaotic motion (determined with MEGNO). The behaviour of the variation of eccentricity seems to be a good indicator for different dynamical regimes, and we verified that for a very thin island with eccentricities e_3 from 0.01 to 0.04 there exists a region of regular orbits.

A representative plane for the Laplace resonance, independent of angular initial conditions, was found. All angles must be set to 0° ($\theta_1 = \theta_2 = \theta_3 = \Delta\varpi_{31} = 0$) but $\Delta\varpi_{32} = 180^\circ$. There exists a strict relation for the mean anomalies, namely $M_1 = 2M_2 = 4M_3$, although not all the values gave stable conditions. In this plane we can observe the real extent of the Laplace resonance.

ACKNOWLEDGEMENTS

Numerical simulations were made using local computing resources (Blafis Cluster) at the University of Aveiro (Aveiro, Portugal).

REFERENCES

Baluev R. V., 2011, Celest. Mech. Dyn. Astron., 111, 235
Batygin K., Morbidelli A., 2013, AJ, 145, 1
Beaugé C., Michtchenko T. A., 2003, MNRAS, 341, 760
Beaugé C., Giuppone C. A., Ferraz-Mello S., Michtchenko T. A., 2008, MNRAS, 385, 2151
Cincotta P. M., Simó C., 2000, A&AS, 147, 205
Cincotta P. M., Giordano C. M., Simó C., 2003, Physica D, 182, 151
Correia A. C. M. et al., 2010, A&A, 511, A21
Ferraz-Mello S., 1979, Dynamics of the Galilean Satellites – An Introductory Treatise. Addison-Wesley, Reading, UK
Gerlach E., Haghighipour N., 2012, Celest. Mech. Dyn. Astron., 113, 35
Giuppone C. A., Tadeu dos Santos M., Beaugé C., Ferraz-Mello S., Michtchenko T. A., 2009, ApJ, 699, 1321
Gladman B., 1993, Icarus, 106, 247
Hadjidemetriou J. D., 2002, Celest. Mech. Dyn. Astron., 83, 141
Kley W., Lee M. H., Murray N., Peale S. J., 2005, A&A, 437, 727
Laughlin G., Chambers J. E., 2001, ApJ, 551, L109
Libert A.-S., Tsiganis K., 2011, Celest. Mech. Dyn. Astron., 111, 201
Lissauer J. J., Ragozzine D., Fabrycky D. C., Steffen J. H., Ford E. A., 2011, ApJS, 197, 8
Lithwick Y., Wu Y., 2012, ApJ, 756, L11
Maffione N. P., Darriba L. A., Cincotta P. M., Giordano C. M., 2011, Celest. Mech. Dyn. Astron., 111, 285
Marchal C., Saari D. G., 1975, Celest. Mech., 12, 115
Morbidelli A., Tsiganis K., Crida A., Levison H. F., Gomes R., 2007, AJ, 134, 1790
Papaloizou J. C. B., Terquem C., 2010, MNRAS, 405, 573
Rivera E. J., Lissauer J. J., 2000, ApJ, 530, 454
Rivera E. J., Laughlin G., Butler R. P., Vogt S. S., Haghighipour N., Meschiari S., 2010, ApJ, 719, 890
Wang S., Ji J., Zhou J.-L., 2012, ApJ, 753, 170

This paper has been typeset from a TEX/LATEX file prepared by the author.